Contrib Mineral Petrol (2008) 155:673–688
DOI 10.1007/s00410-007-0264-y

ORIGINAL PAPER

# Prograde garnet growth along complex *P–T–t* paths: results from numerical experiments on polyphase garnet from the Wölz Complex (Austroalpine basement)

**F. Gaidies · C. de Capitani · R. Abart · R. Schuster**

Received: 31 March 2007 / Accepted: 31 October 2007 / Published online: 28 November 2007


**Abstract** Garnet in metapelites from the Wölz Complex of the Austroalpine crystalline basement east of the Tauern Window characteristically consists of two growth phases, which preserve a comprehensive record of the geothermal history during polymetamorphism. From numerical modelling of garnet formation, detailed information on the pressure–temperature–time (*P–T–t*) evolution during prograde metamorphism is obtained. In that respect, the combined influences of chemical fractionation associated with garnet growth, modification of the original growth zoning through intragranular diffusion and the nucleation history on the chemical zoning of garnet as *P* and *T* change during growth are considered. The concentric chemical zoning observed in garnet and the homogenous rock matrix, which is devoid of chemical segregation, render the simulation of garnet growth through successive equilibrium states reliable. Whereas the first growth phase of garnet was formed at isobaric conditions of ~3.8 kbar at low heating/cooling rates, the second growth phase grew along a Barrovian *P–T* path marked with a thermal peak of ~625°C at ~10 kbar and a maximum in *P* of ~10.4 kbar at ~610°C. For the heating rate during the growth of the second phase of garnet, average rates faster than 50°C $Ma^{-1}$ are obtained. From geochronological investigations the first growth phase of garnet from the Wölz Complex pertains to the Permian metamorphic event. The second growth phase grew in the course of Eo-Alpine metamorphism during the Cretaceous.

**Keywords** Eo-Alpine metamorphism · Equilibrium thermodynamics · Permian metamorphism

## Introduction

Due to slow diffusion within garnet at conditions of low- to medium-grade metamorphism (e.g. Loomis et al. 1985; Chakraborth and Ganguly 1992; Vielzeuf et al. 2007), the compositions that a garnet acquires during growth have high potential to be preserved as chemical zoning. If chemical transport in the rock matrix is fast relative to the rate of garnet growth, successive growth increments may form in thermodynamic equilibrium with the remaining phases present in the rock matrix. In this case, the growth zoning of garnet reflects the equilibrium partitioning of the chemical components between the growing garnet and the rock matrix. As the equilibrium partitioning varies with pressure (*P*) and temperature (*T*), the chemical zoning of garnet bears thermobarometric information on the portion

**Electronic supplementary material** The online version of this article (doi:10.1007/s00410-007-0264-y) contains supplementary material, which is available to authorized users.

Communicated by J. Hoefs.

F. Gaidies · C. de Capitani
Department of Geosciences, University of Basel, Bernoullistrasse 30, 4056 Basel, Switzerland

R. Abart
Institute of Geological Sciences, Free University Berlin, Malteserstrasse 74-100, 12249 Berlin, Germany

R. Schuster
Geological Survey of Austria, Neulinggasse 38, 1031 Vienna, Austria

F. Gaidies (✉)
Department of Geoscience, University of Calgary, Calgary, AB, Canada T2N 1N4
e-mail: fgaidies@ucalgary.ca

of the *P–T* trajectory, over which it was formed (Spear 1993).

Estimates for the *P–T* conditions that prevailed during garnet growth may be obtained from garnet isopleth thermobarometry (Evans 2004; Gaidies et al. 2006; Stowell et al. 2001; Vance and Mahar 1998; Zeh 2001; Zeh and Holness 2003). This technique is based on equilibrium thermodynamic concepts and makes use of the compositional relations between the matrix and the garnet porphyroblast. In garnet isopleth thermobarometry, observed chemical compositions of garnet growth increments in a given volume of rock are compared with garnet compositions that are calculated from phase equilibria for the respective bulk rock composition. Given that mass transport in the rock matrix is fast compared to garnet growth, the composition of the matrix is the thermodynamically relevant bulk composition. Because of the limited efficiency of diffusion within garnet, the chemical components that are incorporated into garnet during growth are effectively removed from the rock matrix. This process is commonly referred to as chemical fractionation (e.g. Hollister 1966; Atherton 1968) and may substantially change the chemical composition of the rock matrix. Therefore, chemical fractionation must be accounted for, if garnet isopleth thermobarometry is to be applied to successive growth increments of a garnet porphyroblast (e.g. Evans 2004; Gaidies et al. 2006).

Garnet isopleth thermobarometry applied to successive garnet growth increments yields information on the *P–T* conditions over the entire interval of garnet growth (Evans 2004; Gaidies et al. 2006). In garnet isopleth thermobarometry it is commonly assumed that diffusion within garnet is infinitely slow so that the original chemical zoning is preserved without modification. In this study we drop the assumption of infinitely slow diffusion within garnet, and we investigate the potential effects of intracrystalline diffusion on the chemical zoning pattern of garnet prophyroblasts.

The efficiency of intragranular diffusion depends on component mobility and the gradients of the respective chemical potentials, where the latter are related to compositional gradients in the growth zoning of garnet. It has been argued by Gaidies et al. (2007) that sharp maxima in manganese concentration may develop in the cores of garnet porphyroblasts that nucleate late during a metamorphic event. Such sharp maxima are effectively degraded by the diffusive loss of manganese from the core region. If garnet isopleth thermobarometry is applied to such regions of a garnet this may systematically overestimate *T*, because—for a given bulk rock composition—the spessartine content of garnet is very sensitive to *T*.

Large compositional gradients in garnet also occur at those growth increments that coincide with changes in the thermodynamically stable mineral assemblage (Gaidies et al., 2007). Such changes in paragenesis may occur repeatedly throughout the entire garnet growth history so that modification of the original growth zoning by intragranular diffusion needs to be considered all over a garnet porphyroblast. As envisaged by Spear (1988), although rather inefficient, intragranular diffusion may lead to a flux of components between garnet and the rock matrix. Similar to garnet fractionation but in a complementary fashion, this may modify the thermodynamically relevant bulk rock composition. This effect was referred to as "internal metasomatism" by Spear (1988).

We use the software program THERIA_G (Gaidies et al., 2007) for forward modelling of garnet growth. This tool allows to account simultaneously for the requirements of thermodynamic equilibrium between the garnet rim and the rock matrix, chemical fractionation during garnet growth, modification of the original growth zoning through intragranular diffusion, as well as the nucleation history. We apply this technique to unravel the polymetamorphic history of garnet from the Austroalpine crystalline basement. We obtain constraints on the *P–T–t* trajectories of a Permian and a Cretaceous metamorphic event from modelling the chemical zoning of two distinct growth phases of garnet. The model *P–T–t* paths are compared with information on the geothermal history constrained by independent petrological and geochronological data. Finally, an often perceived feature of the growth zoning of polymetamorphic garnet from the Austroalpine crystalline basement is presented, which may be used as a rock-specific geothermobarometer.

## Geological background

The rock sample, which is investigated in the present study, was taken from the Wölz Complex, a prominent lithostratigraphic unit of the Upper Austroalpine basement nappes in the Eastern Alps (Schmid et al. 2004). The Austroalpine nappe system represents the frontal part of the Apulian continental microplate, which underwent internal deformation due to an intracontinental collision event during the Cretaceous. The Wölz Complex was part of the tectonic lower plate and experienced a greenschist to amphibolite facies metamorphic overprint during the Cretaceous subduction event. Because of Cretaceous metamorphism, which is referred to as Eo-Alpine metamorphism, low- to medium-grade metamorphic assemblages of pre-Cretaceous origin have been largely obliterated (Gaidies et al. 2006; Schuster and Frank 1999; Schuster et al. 2004, 2001; Schuster and Thöni 1996).

The polymetamorphic history of the Wölz Complex is documented by garnet porphyroblasts with two distinct growth phases (Abart and Martinelli 1991; Bernhard and Hoinkes 1999; Faryad and Chakraborty 2005; Faryad and Hoinkes 2003; Gaidies et al. 2006; Schuster and Frank 1999; Schuster et al. 2001; Schuster and Thöni 1996). The oldest garnet growth phase forms the cores of the garnet porphyroblasts and is separated from the younger garnet growth phase by a microstructural and compositional discontinuity. From radiometric dating of garnet from the Wölz Complex it is known that the first growth phase grew during a Permian metamorphic event, and the second growth phase was formed in the course of Cretaceous metamorphism (Schuster and Frank 1999; Schuster and Thöni 1996; Sölva et al. 2001; Thöni 2002).

The studied rock sample is a garnet-bearing metapelite from the Schöttelbach area. For a detailed description of the geographical position and more information on the regional geology, the reader is referred to a previous study (Gaidies et al. 2006).

## Petrological and geochronological constraints on the geothermal history of the Wölz Complex

The cores of the oldest garnets represent the earliest testimony of metamorphism in the rocks from the Wölz Complex. They were subject to several geochronological and thermobarometrical studies. Using the Sm–Nd garnet–whole-rock method, an age of 269 ± 4 Ma was obtained for garnet that forms the cores of polyphase garnet porphyroblasts (Schuster and Thöni 1996; Schuster and Frank 1999; Thöni 2002). Permian metamorphism in the Austroalpine basement occurred in an extensional tectonic regime. This is indicated by magmatic activity as well as high-temperature/low-pressure (*HT/LP*) metamorphic assemblages and the continuous peneplanation of the surface topography as inferred from the sedimentary record (Schuster et al. 2001). Lithospheric extension probably started at ~290 Ma, and the thermal peak was reached at ca. ~260 Ma.

Phengite thermobarometry (Feenstra 1996; Franz et al. 1977) applied to monomineralic inclusions of margarite, paragonite, and muscovite in the Permian growth phase of garnet from the Wölz Complex (Schuster and Frank 1999) yielded *T* conditions of lower greenschist facies at low *P* (Schuster et al. 2001). According to Gaidies et al. (2006) incipient garnet growth during the Permian occurred at 535 ± 20°C and 4.0 ± 0.5 kbar in rock samples from the Schöttelbach area [*P–T–t* point (1) in Fig. 1]. From the observed *P–T* conditions a geothermal gradient of ~40°C km$^{-1}$ can be calculated supporting the hypothesis of a Permian extensional event for this part of the Austroalpine basement. However, the heating rate associated with the respective pre-Eo-Alpine metamorphic event as well as the peak conditions of Permian metamorphism in the Wölz Complex are not yet known.

From the Late Permian to the Early Jurassic more than 3,000 m of shallow water sediments were deposited on the slowly subsiding Austroalpine crust (Mandl 2000; Tollmann 1985). Due to intense overprint in the course of Eo-Alpine metamorphism, this part of the geothermal history is not documented in metapelites of the Wölz Complex. However, for Austroalpine units which reached similar metamorphic conditions during the Permian metamorphic event but were less intensely affected during the Cretaceous, K–Ar muscovite ages (reflecting cooling below ~420°C) in the range of 240–210 Ma [*P–T–t* point (2) in Fig. 1] are characteristic (Schuster et al. 2001). Therefore, a geothermal gradient of ~25°C km$^{-1}$ can be assumed for the respective period in the geothermal history.

In the Valanginian (~137 Ma) the Permomesozoic sediments were sheared off from the future Koralpe-Wölz nappe system and the subduction of basement rocks started

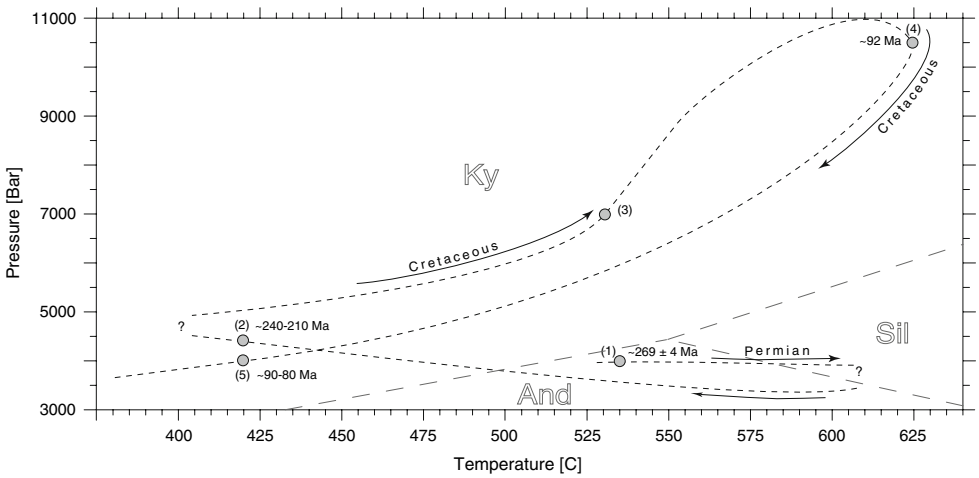


**Fig. 1** Compilation of geochronological and thermobarometrical data (marked with *points*) obtained from rocks of the Wölz Complex (Schuster and Thöni 1996; Schuster and Frank 1999; Thöni 2002, 2006; Schuster et al. 2001; Sölva et al. 2001; Faryad and Hoinkes 2003; Hejl 1984; Gaidies et al. 2006). For explanation see text

within the Eo-Alpine intracontinental subduction zone (Schmid et al. 2004). The application of isopleth thermobarometry to garnet, which grew during the Eo-Alpine metamorphic event, yielded 540 ± 10°C and 6.5 ± 0.5 kbar for the stage of incipient garnet growth [*P–T* point (3) in Fig. 1] in metapelites from the Schöttelbach region (Gaidies et al. 2006).

For samples from similar geographical positions, conditions of 600–650°C at 10–11 kbar were determined by Faryad and Hoinkes (2003) for the metamorphic peak at ~92 Ma (Thöni 2006) [*P–T–t* point (4) in Fig. 1]. From these *P–T* estimates, a geothermal gradient of ~20°C $km^{-1}$ is calculated. The markedly low geothermal gradient points to fast subduction during the Cretaceous, where thermal relaxation could not keep up with rapid *P* increase. After the metamorphic peak the rocks of the Koralpe-Wölz nappe system were exhumed in a metamorphic extrusion wedge (Schmid et al. 2004) and typical K–Ar and Rb–Sr cooling ages on micas are 90–80 Ma (Hejl 1984) [*P–T–t* point (5) in Fig. 1]. From diffusion modelling in polyphase garnet porphyroblasts of the Wölz Complex, Faryad and Chakraborty (2005) suggest a duration of ~0.8–0.9 Ma from *P–T* conditions similar to point (3) in Fig. 1 to *P–T* conditions of ~540°C and 4 kbar along the retrograde part of the Cretaceous *P–T–t* trajectory. For the metamorphic peak of Eo-Alpine metamorphism in the Wölz Complex, Faryad and Chakraborty (2005) considered conditions of ~590°C at 10 kbar. According to apatite fission track ages obtained by Hejl (1998), final cooling below ~100°C occurred in the Miocene at 15–20 Ma.

## Methods

### Sample preparation, EPMA, combustion analysis, and WDXRFA

The rock sample 12F03, which is investigated in the present study, was also subject to previous research (Gaidies et al. 2006). Serial sections with a spacing of ~0.6–0.8 mm were prepared from the largest garnet in a representative sample domain of ~1 × 2 × 3 $cm^3$. The aim of this procedure was to obtain a cross-section of garnet, which contains the entire garnet growth history.

Electron probe micro-analysis (EPMA) was done on a JEOL JXA-8200 at ETH Zurich. The accelerating voltage was 15 kV for a beam current of 10 nA. X-ray maps and the compositional profiles of garnet were produced for Mn, Fe, Mg, and Ca. The X-ray maps as well as the respective compositional profile, which intersects the garnet core and thus contains the most information on garnet growth history, are shown in Figs. 2 and 3.

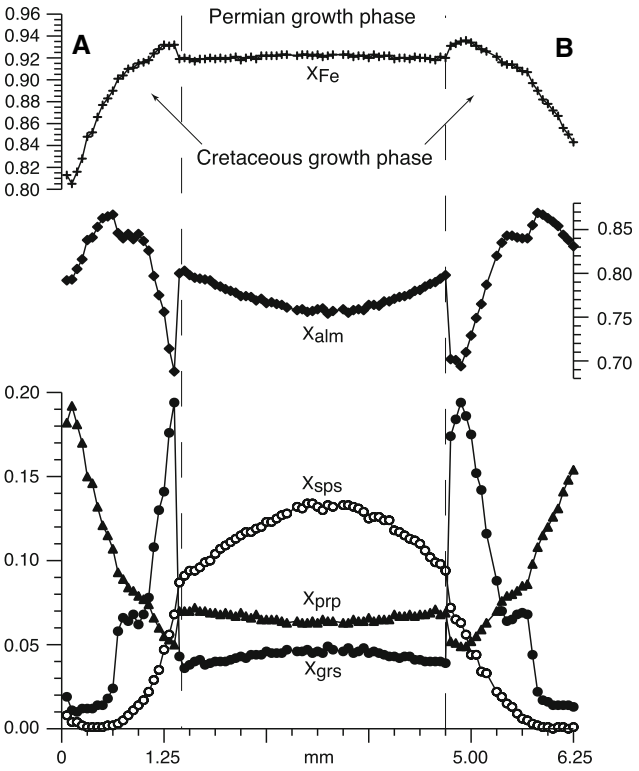


**Fig. 2** Compositional profile intersecting the centre of the largest garnet porphyroblast in a representative domain of rock sample 12F03

Combustion analysis and wavelength-dispersive X-ray fluorescence analysis (WDXRFA) were done to obtain the major element composition of the rock sample. For the combustion analysis, a LECO combustion analyser was used. WDXRFA was carried out on a glass pellet prepared from a rock sample of ~1 kg employing a Bruker AXS SRS-3400 at Basel University. The bulk rock composition obtained for the sample investigated in the present study is given in Table 1.

### Numerical modelling of prograde garnet growth

The bulk rock composition of sample 12F03 (Table 1) was used as the thermodynamically relevant bulk composition for the stage of incipient garnet growth. For thermodynamic calculations in the simplified model system MnO–$Na_2O$–CaO–$K_2O$–FeO–MgO–$Al_2O_3$–$SiO_2$–$H_2O$–$TiO_2$, the database of Holland and Powell (1998) (thermodynamic database of THERMOCALC, version 3.21) was used [for detailed information on the solution models and notations used in the current study, the reader is referred to the companion paper (Gaidies et al., 2007)]. Rock-specific equilibrium assemblage diagrams were calculated with program DOMINO (de Capitani 1994, see also: http://titan.minpet.unibas.ch/minpet/theriak/theruser.html).

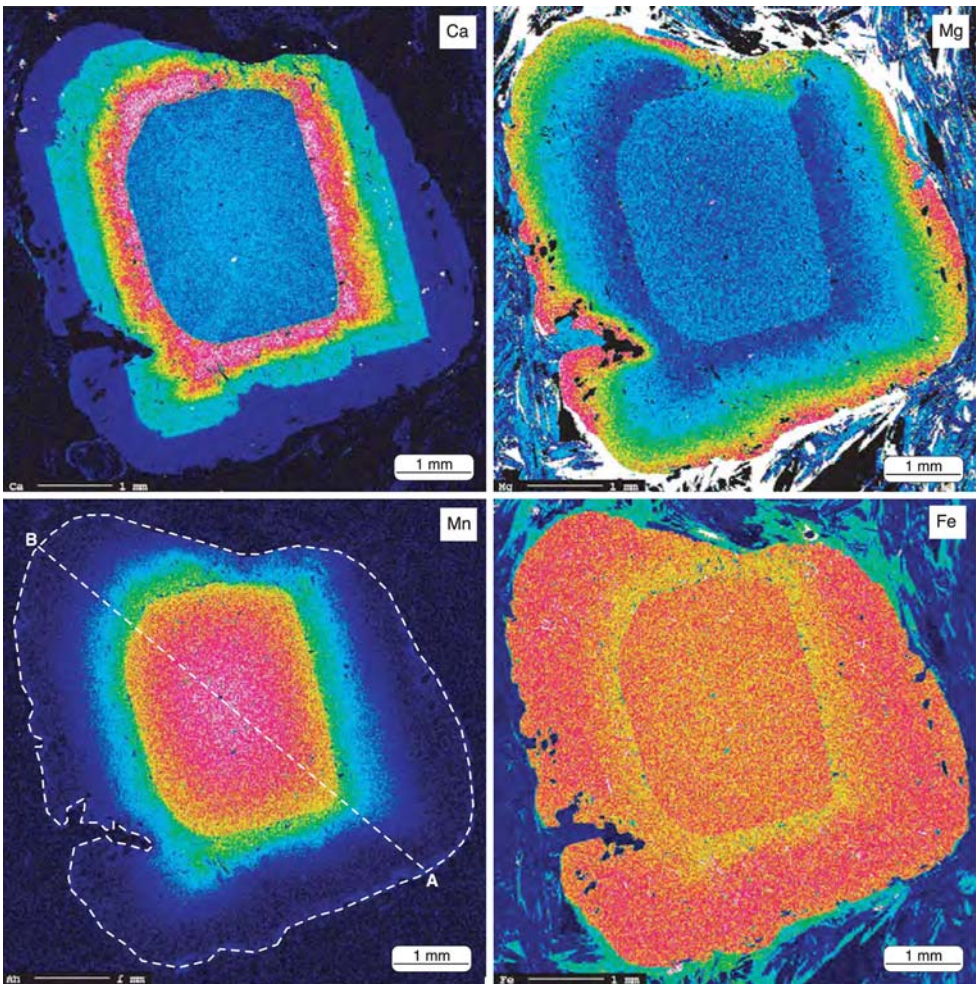


**Fig. 3** X-ray maps of a garnet porphyroblast of a representative domain of rock sample 12F03. The location of the compositional profile *A–B* as illustrated in Fig. 2 is shown

In garnet growth simulations, $H_2O$ and $SiO_2$ are considered as excess components to account for the presence of quartz and an aqueous fluid throughout the entire *P–T* range of interest.

The kinetic parameters of Chakraborty and Ganguly (1992) were applied to model intragranular diffusion in garnet. Small graphite inclusions are very abundant in the garnet porphyroblast investigated in this study indicating coexistence with a graphite saturated fluid. This is why the kinetic data of Chakraborty and Ganguly (1992), which were obtained with graphite present, could be employed without modification. In a previous study (Gaidies et al. 2006) it was shown that the influence of changing $H_2O$ and $CO_2$ activities on garnet composition and stability is minor for the sample studied and decreases with increasing *P*. Therefore, in the present study, pure $H_2O$ was considered as fluid phase.

## Sample description

A detailed description of the petrography and garnet chemistry of sample 12F03 can be found in Gaidies et al. (2006). In the following only a brief summary is given.

### Petrography

The rock sample investigated in the present study is a metapelite with garnet porphyroblasts, which consist of two distinct growth phases. A first growth phase, which forms the cores of the porphyroblasts, can easily be distinguished from the rim-forming second phase based on abundant ilmenite and graphite inclusions that are concentrated at the boundary between both zones. From the microstructural relationship to the main schistosity it is

**Table 1** Bulk rock composition of sample 12F03 (wt%)

| $SiO_2$ | $TiO_2$ | $Al_2O_3$ | $Fe_2O_3$ | MnO | MgO | CaO | $Na_2O$ | $K_2O$ | $H_2O$ | $CO_2$ | $\sum$ |
|---|---|---|---|---|---|---|---|---|---|---|---|
| 57.51 | 1.19 | 20.98 | 9.48 | 0.11 | 2.28 | 0.46 | 1.23 | 3.73 | 2.75 | 0.44 | 100.16 |

inferred that the second garnet growth phase grew synchronously to the formation of the foliation.

The rim of garnet of sample 12F03 is marked by inclusions of quartz, muscovite, ilmenite, rutile and tourmaline and is strongly pigmented with graphite. It is interesting to note that the abundance of rutile inclusions rises towards the outer portions of the rim, whereas the abundance of ilmenite decreases. In a similar fashion, the intensity of graphite pigmentation decreases from the inner portions of the rim outwards. Whereas the rim of the garnet porphyroblast investigated in the present study is approximately 1.5 mm wide, the first growth phase is about 4 mm in diameter. It contains ilmenite, quartz, tourmaline as well as small muscovite grains as mineral inclusions. The polyphase garnet porphyroblasts are enclosed by a fine-grained matrix composed of muscovite, quartz, tourmaline, biotite, ilmenite, rutile as well as plagioclase and retrograde chlorite. The foliation of the rock is formed by muscovite and tourmaline and minor biotite, rutile and ilmenite. Chlorite and a second biotite generation are often observed as replace products of the second garnet growth phase. Static grown small biotite flakes crosscutting the rock foliation could also be perceived.

### Garnet chemistry

The garnet porphyroblasts of rock sample 12F03 are strongly zoned with respect to $X_{sps}$ [= $Mn/(Fe^{2+} + Ca + Mg + Mn)$], $X_{alm}$ [= $Fe^{2+}/(Fe^{2+} + Ca + Mg + Mn)$], $X_{prp}$ [= $Mg/(Fe^{2+} + Ca + Mg + Mn)$], and $X_{grs}$ [= $Ca/(Fe^{2+} + Ca + Mg + Mn)$] (Figs. 2, 3). The chemical zoning patterns (Fig. 3; see also Fig. 5 of Gaidies et al. 2006) exhibit an almost euhedral shape indicating that the original zoning was preserved and resorption occurred mainly subsequent to the formation of the second growth phase. The boundary between first and second growth phase can easily be discerned from a sharp increase of $X_{grs}$ by ~13.5 mol% and a concomitant decrease of $X_{alm}$ by ~9.5 mol%. The boundary between first and second growth phase is also marked by a sudden decrease of $X_{sps}$ by ~2.5 mol% (Fig. 2).

The first growth phase is characterized by a continuous outwards decrease of $X_{sps}$ and $X_{grs}$ and a concomitant increase of $X_{alm}$ and $X_{prp}$. A 'shoulder' in the $X_{grs}$ profile forms a conspicuous feature in the central part of the second growth phase. $X_{grs}$ decreases sharply from this shoulder outwards and, finally, reaches a constant value of ~0.015 in the outermost 0.3 mm of the garnet rim. In a similar fashion, a 'step' in the $X_{alm}$ profile is observed. Whereas $X_{grs}$ decreases sharply from the shoulder outwards, $X_{alm}$ increases and reaches a maximum of ~0.87 within the garnet of the second growth phase. From the location of maximum $X_{alm}$ outwards the almandine content decreases continuously.

In the outermost tens of micrometres of the garnet rim $X_{grs}$, $X_{sps}$, and $X_{Fe}$ [=Fe/(Fe + Mg)] increase, and the $X_{prp}$ decreases concomitantly. This feature is only locally developed.

## Results

To extract geothermobarometric information from the chemical zoning pattern of the entire garnet porphyroblast garnet growth was simulated for various *P–T–t* trajectories and different theoretical garnet crystal size frequency distributions (CSD). In this communication, the most successful results of the garnet growth simulations are presented. In that respect, firstly the *P–T* path and garnet CSD was determined, along which the garnet growth simulations yield the best fit with the observed garnet chemical patterns. In a second step, the influence of intragranular diffusion on garnet and effective bulk rock composition was considered linking the *P–T* trajectory to different heating and cooling scenarios.

Because the garnet porphyroblasts of rock sample 12F03 are very coarse-grained, an enormous preparational effort would have to be undertaken to obtain a garnet CSD-analysis with sufficient statistical significance. This could not be done in our study. For practical purposes, a theoretical CSD with a polymodal size-frequency distribution was applied (Fig. 4) that accounts for crystallization during the Permian and the Cretaceous metamorphic events.

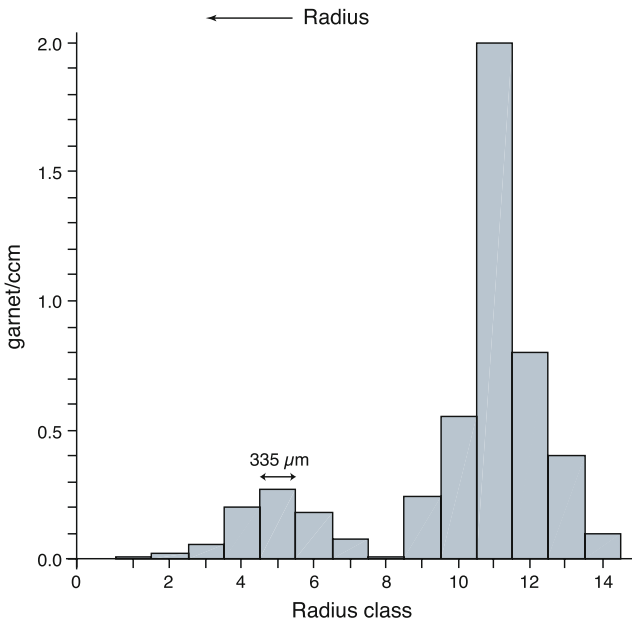


**Fig. 4** Theoretical relative garnet crystal size frequency distribution used for garnet growth simulation

For the Permian event the CSD (radius classes 1 to 8 in Fig. 4) was chosen in such a way that the garnet individuals of radius class 4 have similar size as the first garnet growth phase of sample 12F03. This is motivated by the notion that the garnet investigated probably pertains to a relatively large size class but almost certainly is not the largest individual of the first growth phase that was formed in a larger rock volume with similar composition as the investigated sample. The specific size-frequency distribution of garnet crystals that originate from the second metamorphic cycle (radius classes 9 to 14 in Fig. 4) was chosen so that the simulated size of the second growth phase on individuals of radius class 4 (of the first growth phase) matches the size of the respective individual in sample 12F03. Garnet individuals of radius classes 9–14 are single-phase porphyroblasts, the nucleation and growth of which entirely pertains to Cretaceous metamorphism.

## The original garnet growth zoning

Figure 5 illustrates the calculated compositional profile of garnet from size class 4 (Fig. 4), which results from growth along *P–T* path A (Fig. 7). The chemical patterns shown in Fig. 5 were calculated from equilibrium phase relations taking into account the effect of chemical fractionation during garnet growth. Intragranular diffusion was not considered so that the calculated compositional profile represents pure garnet growth zoning. In addition, Fig. 5 shows the equilibrium assemblages that correspond to the respective garnet growth increments. The calculated equilibrium phase relations for the time of incipient garnet growth in rock sample 12F03 are illustrated in Fig. 6.

The garnet growth simulation clearly shows that changes in the thermodynamically stable equilibrium assemblage during garnet growth produce marked changes in the chemical gradients within the growth zoning of garnet (Fig. 5). Our calculations indicate that most of the first garnet growth phase grew in equilibrium with plagioclase, ilmenite, chloritoid, chlorite, phengite, as well as with staurolite, quartz, and $H_2O$ (assemblage 2 in Fig. 5). It is interesting to note that this assemblage is stable only over a fairly small *P–T* range (Fig. 6).

In general, the compositional profiles obtained from garnet growth modelling are very sensitive to the choice of the *P–T* path. In particular, for the bulk rock composition of sample 12F03, $X_{grs}$ of the first garnet growth increment is strongly contingent on *P*. $X_{grs}$ observed in garnet of rock sample 12F03 (Fig. 2) constrains *P* to ~3.8 kbar during the incipient stages of Permian garnet growth. If a *P–T* path was chosen that exceeds the applied trajectory by ~1 kbar, this would lead to an increase in $X_{grs}$ by ~0.03 during initial garnet growth. This is beyond the analytical uncertainty.

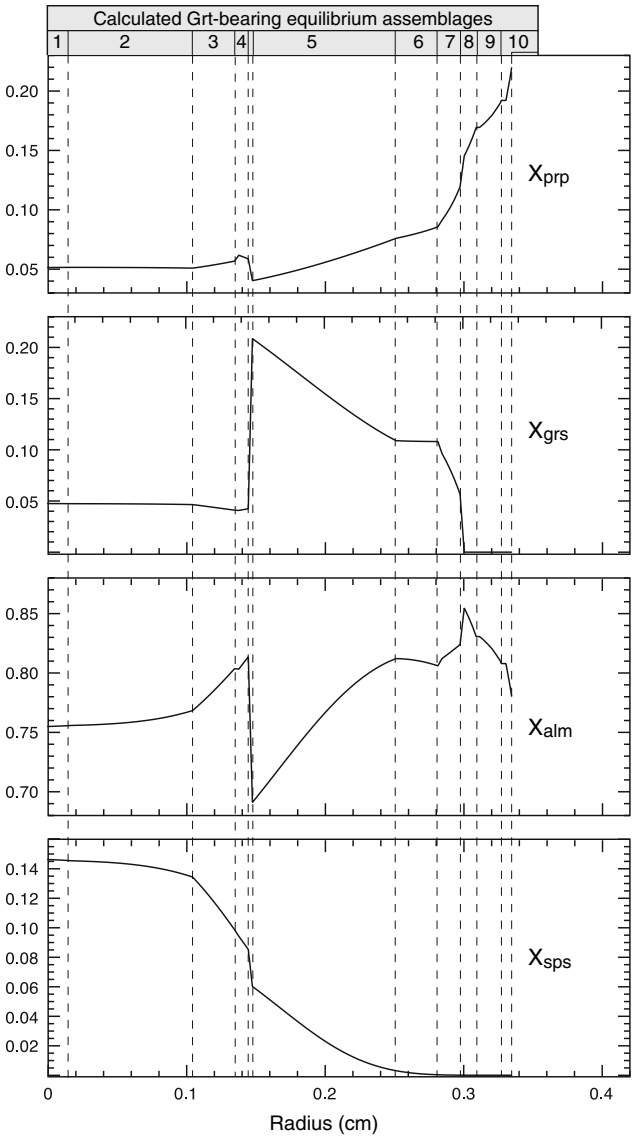


**Fig. 5** Calculated compositional profile of garnet in rock sample 12F03 neglecting the influence of intragranular diffusion on garnet and effective bulk rock composition. Garnet growth simulation was performed along *P–T* path A (Fig. 7, Appendix of Electronic supplementary material) using a bimodal CSD (Fig. 4). The profile was calculated for garnet of radius class 4. All equilibrium assemblages contain $H_2O$ and Qtz (*2* Phng corresponds to unmixing of Phng into a paragonite- and muscovite-rich phase)

The first *P–T* loop was chosen to represent the *HT-LP* Permian metamorphic event. In the garnet growth simulation, garnet growth during the Permian event ceases at the

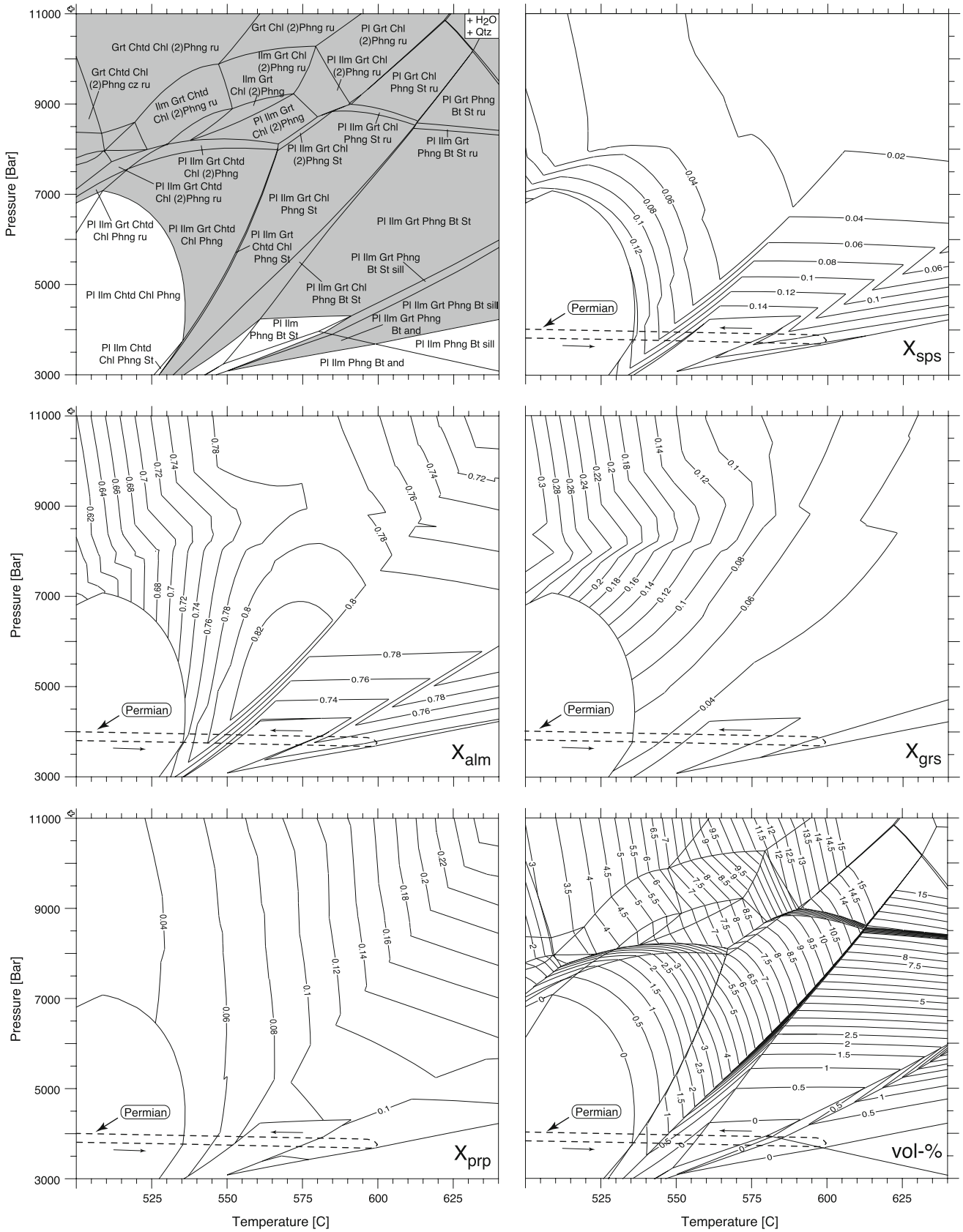
Pressure [Bar]
Temperature [C]
+ H2O
+ Qtz
Grt Chl (2)Phng ru
Grt Chtd Chl (2)Phng ru
Grt Chtd Chl (2)Phng cz ru
Ilm Grt Chl (2)Phng ru
Ilm Grt Chtd Chl (2)Phng ru
Ilm Grt Chl (2)Phng
Pl Ilm Grt Chl (2)Phng ru
Pl Grt Chl (2)Phng ru
Pl Grt Chl Phng St ru
Pl Grt Phng Bt St ru
Pl Ilm Grt Chl Phng St ru
Pl Ilm Grt Phng Bt St ru
Pl Ilm Grt Chtd Chl (2)Phng
Pl Ilm Grt Chtd Chl (2)Phng ru
Pl Ilm Grt Chl (2)Phng St
Pl Ilm Grt Chl Phng St
Pl Ilm Grt Phng Bt St
Pl Ilm Grt Chtd Chl Phng ru
Pl Ilm Grt Chtd Chl Phng
Pl Ilm Grt Chtd Chl Phng St
Pl Ilm Grt Phng Bt St sill
Pl Ilm Chtd Chl Phng
Pl Ilm Grt Chl Phng Bt St
Pl Ilm Grt Phng Bt St sill
Pl Ilm Phng Bt St
Pl Ilm Grt Phng Bt and
Pl Ilm Phng Bt sill
Pl Ilm Chtd Chl Phng St
Pl Ilm Phng Bt and
Permian
Xsps
Xalm
Xgrs
Xprp
vol-%

◀ **Fig. 6** Initial equilibrium phase relations and dependency of garnet chemistry and garnet volume on *P–T* for the bulk rock chemistry of sample 12F03 (Table 1). $H_2O$ and $SiO_2$ are considered as excess components throughout the respective *P–T* space. In addition, the Permian part of *P–T* path A, which is used for garnet growth simulation, is shown (for the detailed *P–T* values, see Appendix of Electronic supplementary material)

*P–T* conditions where biotite enters the stable equilibrium assemblage. The position of the isopleths that represent *P–T* conditions of constant garnet modes drastically change as the biotite-bearing equilibrium assemblage becomes thermodynamically stable (Fig. 6). Consequently, for this specific *HT-LP* trajectory, garnet growth ceases when biotite becomes stable. However, for the retrograde part of the Permian *P–T* path, THERIA_G modelling predicts garnet growth in equilibrium with biotite and staurolite (assemblage 4 in Fig. 5). It is interesting to note that such an equilibrium assemblage would not form if garnet grew along a clockwise *P–T* path.

The equilibrium phase relations and the garnet chemistry calculated for incipient garnet growth in the Cretaceous applying *P–T* path A and neglecting the influences of intragranular diffusion on garnet and effective bulk rock composition are illustrated in Fig. 7. The size of the garnet stability field is reduced in comparison with the initial equilibrium phase relations prior to garnet growth (Fig. 6). This is due to the influence of chemical fractionation associated with garnet growth during the first metamorphic cycle on thermodynamic effective bulk rock composition.

The second *P–T* cycle is modelled to exemplify the geothermal history of the Cretaceous Eo-Alpine metamorphic event. Incipient garnet growth in the course of the Cretaceous event occurs at ~530°C and ~7.6 kbar. As a result, at the boundary between first and second growth phase of garnet an increase in $X_{grs}$ by ~15 mol% is produced as well as a decrease in $X_{sps}$, $X_{alm}$, and $X_{prp}$ by ~2, 12, and 2 mol%, respectively.

From garnet growth simulations with THERIA_G it is evident that during the Cretaceous metamorphic cycle the metapelite followed a *P–T* trajectory, which intersects the stability field of the equilibrium assemblage plagioclase, ilmenite, garnet, chloritoid, chlorite, (2)phengite (muscovite and paragonite), quartz, and an aqueous fluid (marked in Fig. 7). The position and shape of the $X_{grs}$ and $X_{alm}$ isopleths in the corresponding *P–T* field are such that during the growth along such a *P–T* trajectory a shoulder in $X_{grs}$ and a local maximum in $X_{alm}$ are formed. For the bulk rock composition at hand, this is a unique feature. There is no alternative assemblage, in which the garnet chemistry changes similarly with *P–T*. Garnet growth simulations along *P–T* paths, which intersect the same assemblage but correspond to smaller geothermal gradients as illustrated in Fig. 7 result in a broader $X_{grs}$ shoulder with significantly higher values of $X_{grs}$.

Whereas at *P–T* conditions of ~586°C and 9.1 kbar garnet disappears from the equilibrium assemblage, which consists of plagioclase, ilmenite, garnet, chlorite, (2)phengite, quartz, and $H_2O$ (assemblage 7 in Fig. 5), at conditions of ~595°C and 9.6 kbar the equilibrium assemblage ilmenite, garnet, chlorite, (2)phengite, staurolite, quartz, and $H_2O$ (assemblage 8 in Fig. 5) and a maximum in $X_{alm}$ is formed at a later stage along the *P–T* trajectory. That is, along the prograde part of the Cretaceous *P–T* path, a period of garnet instability is calculated spanning ~10°C and 0.5 kbar. During the last stages of garnet formation, THERIA_G modelling yields an outermost rim of ~0.4 mm width, where the second garnet growth phase has extremely low $X_{sps}$ and $X_{grs}$.

The equilibrium phase relations calculated for a thermodynamically relevant bulk composition that is representative for the stage subsequent to garnet growth are displayed in Fig. 8. From Fig. 8 it is evident that for further growth of garnet the rock would have to follow a *P–T* path that reaches at least upper amphibolite facies conditions. Because Mn and Ca have been completely fractionated into garnet during earlier growth stages, the equilibrium phase assemblages are devoid of ilmenite and plagioclase.

## Influence of intragranular diffusion on garnet growth zoning

The *P–T* conditions, at which garnet growth ceases along the prograde part of the Permian *P–T* path (Fig. 6), do not necessarily correspond to the peak conditions of Permian metamorphism. In order to evaluate the influence of the possible peak conditions during Permian metamorphism on garnet composition, garnet growth is modelled along different *P–T–t* loops while the influence of intragranular diffusion in garnet on garnet and on effective bulk rock composition is taken into account. The *P–T–t* loops employed differ with respect to the thermal maximum reached during the Permian. Whereas for *P–T–t* path A$^{\star}$ a thermal maximum of 600°C is considered, for *P–T–t* path B 650°C and for loop C 675°C are applied (Appendix of Electronic supplementary material).

In all cases, garnet growth is modelled with 3 and 100°C $Ma^{-1}$ for the Permian and Cretaceous heating rates, respectively. For the cooling rates −3 and −100°C $Ma^{-1}$ were used for Permian and Cretaceous metamorphism, respectively. In general, a prolonged residence of a rock at elevated *P–T* conditions has a similar effect as slow heating/cooling rates with respect to the efficiency of intragranular diffusion. However, the induced flux between garnet and rock matrix may modify the equilibrium phase

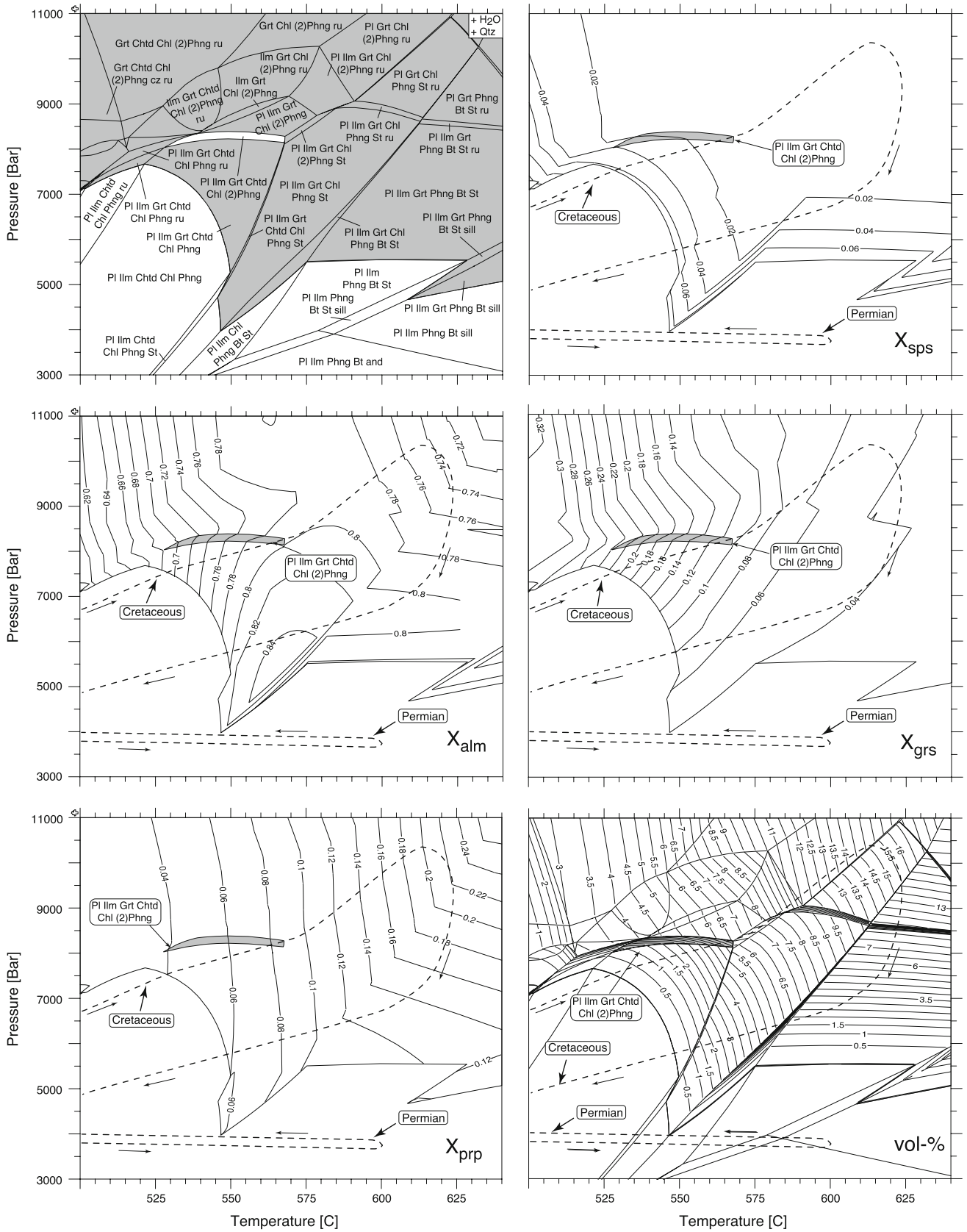
Pressure [Bar]
Temperature [C]
+ H2O
+ Qtz
Grt Chl (2)Phng ru
Pl Grt Chl (2)Phng ru
Grt Chtd Chl (2)Phng ru
Grt Chtd Chl (2)Phng cz ru
Ilm Grt Chl (2)Phng ru
Pl Ilm Grt Chl (2)Phng ru
Pl Grt Chl Phng St ru
Pl Grt Phng Bt St ru
Ilm Grt Chtd Chl (2)Phng ru
Ilm Grt Chl (2)Phng
Pl Ilm Grt Chl (2)Phng
Pl Ilm Grt Chl Phng St ru
Pl Ilm Grt Phng Bt St ru
Pl Ilm Grt Chtd Chl Phng ru
Pl Ilm Grt Chl (2)Phng St
Pl Ilm Grt Chtd Chl (2)Phng
Pl Ilm Grt Chl Phng St
Pl Ilm Grt Phng Bt St
Pl Ilm Chtd Chl Phng ru
Pl Ilm Grt Chtd Chl Phng ru
Pl Ilm Grt Chtd Chl Phng
Pl Ilm Grt Chtd Chl Phng St
Pl Ilm Grt Chl Phng Bt St
Pl Ilm Grt Phng Bt St sill
Pl Ilm Chtd Chl Phng
Pl Ilm Phng Bt St
Pl Ilm Phng Bt St sill
Pl Ilm Grt Phng Bt sill
Pl Ilm Chtd Chl Phng St
Pl Ilm Chl Phng Bt St
Pl Ilm Phng Bt sill
Pl Ilm Phng Bt and
Pl Ilm Grt Chtd Chl (2)Phng
Cretaceous
Permian
$X_{sps}$
$X_{alm}$
$X_{grs}$
$X_{prp}$
vol-%

◀ **Fig. 7** Equilibrium phase relations and dependency of garnet chemistry and garnet volume on *P–T* for the time of incipient garnet growth during the Cretaceous. The influence of diffusional relaxation in garnet on effective chemical composition is not taken into account. $H_2O$ and $SiO_2$ are considered as excess components throughout the respective *P–T* space. In addition, *P–T* path A that was used for garnet growth simulation is shown (for the detailed *P–T* values, see Appendix of Electronic supplementary material). The equilibrium assemblage is marked, which has to be intersected by the *P–T* path to form a shoulder in $X_{grs}$ and a local maximum in $X_{alm}$

relations and has, therefore, to be considered. For the rock sample investigated in this study, variable heating/cooling rates and a prolonged residence have a negligible influence on the chemical composition of the garnet porphyroblast.

The compositional profile of garnet from radius class 4 (Fig. 4) calculated for garnet growth along *P–T–t* loop A$^{\star}$ largely resembles the chemical composition of garnet computed for the growth along *P–T–t* path B and C (Fig. 9). Garnet growth up to 650°C (loop B) results in more shallow compositional gradients in the first growth phase of the polyphase garnet crystal than for the growth up to 600°C (loop A$^{\star}$). However, the calculated chemical gradients of all components for both, *P–T–t* trajectories A$^{\star}$ and B, are somewhat gentler in the core region and steeper in the outer portions of the Permian growth phase compared with the observed compositional gradients (Fig. 9). This feature is more pronounced for $X_{sps}$ and $X_{alm}$ than for $X_{grs}$ and $X_{prp}$. The systematic discrepancy between observed and modelled compositional gradients suggests that the original growth zoning was degraded by intracrystalline diffusion to a larger extent than accounted for in the model.

The garnet growth simulation applying a maximum *T* of 675°C during the Permian (loop C) yields a compositional

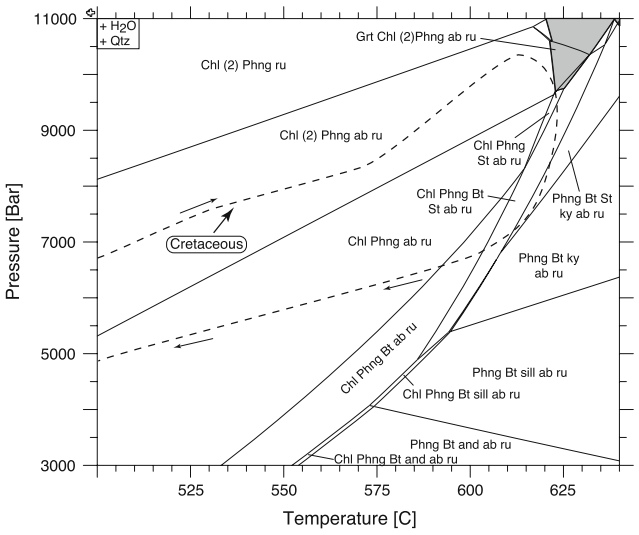


**Fig. 8** Equilibrium phase relations subsequent to garnet growth. The influence of intragranular diffusion in garnet on thermodynamic effective bulk rock composition is not considered

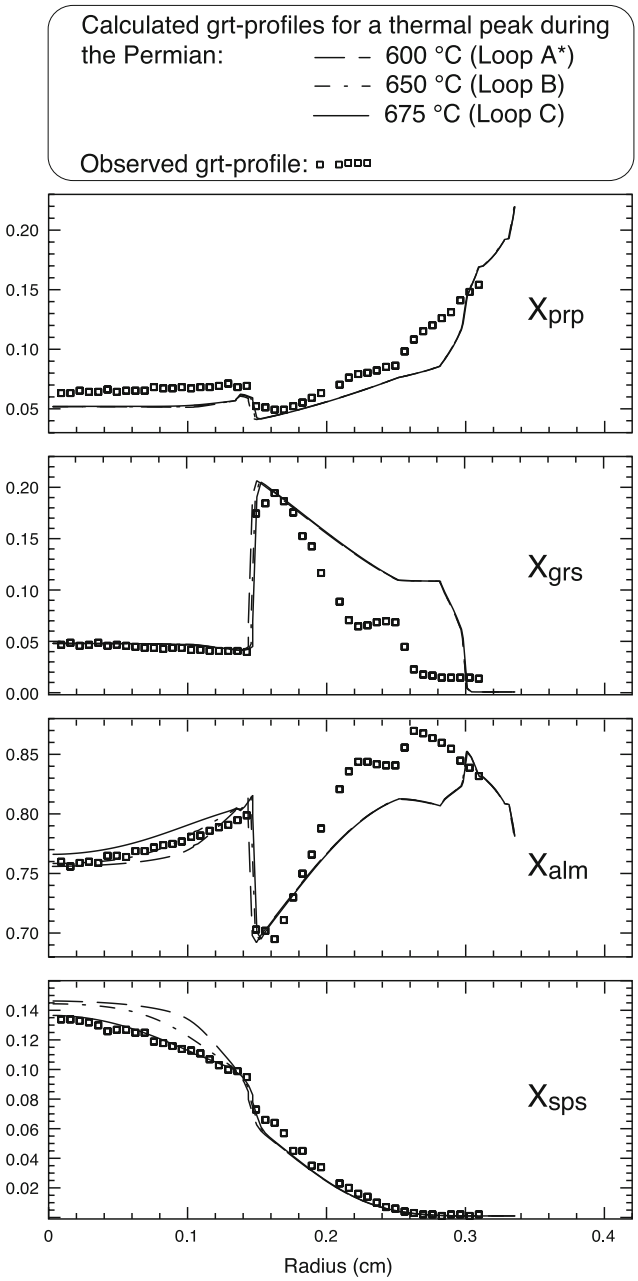


**Fig. 9** Compositional profiles of garnet from radius class 4 (Fig. 4) calculated for different peak conditions during the Permian metamorphic event. For the Permian heating/cooling rate $\pm$ 3°C $Ma^{-1}$ and for Eo-Alpine metamorphism $\pm$100°C $Ma^{-1}$ are considered. See the Appendix of Electronic supplementary material for detailed values of the *P–T–t* loops. The *symbols* correspond to the observed compositional profile to the right-hand side of the core in Fig. 2

pattern for the first garnet growth phase that matches the observed chemical gradients fairly well (Fig. 9). In that case, the only difference between predicted and observed garnet composition is in the calculated contents of $X_{alm}$ and $X_{prp}$ which differ from the observed quantities by an almost uniform value of $\sim$0.01 and $\sim -0.01$, respectively.

Results that are obtained, if *P–T* path A (Fig. 6) is linked to a heating rate of 1°C $Ma^{-1}$ for the Permian metamorphic cycle, where during the retrograde part of the *P–T* path the rate increases to $\sim -150$°C $Ma^{-1}$ (Appendix of Electronic supplementary material) yield a compositional profile of garnet from radius class 4, which is rather similar to the chemical pattern acquired for growth along *P–T–t* loop A☆ (Fig. 9).

For modelling the chemical zoning of the Cretaceous garnet growth phase, *P–T* path A (Fig. 7) was applied. The results obtained for different heating rates are illustrated in Fig. 10. The most prominent features of the chemical zoning are nicely reproduced, at least in a qualitative sense. Nevertheless, remarkable differences between calculated and observed garnet composition can be perceived.

Even though a shoulder in $X_{grs}$ as well as a concomitant local maximum in $X_{alm}$ are simulated, their specific positions in garnet differ from the positions, at which they are observed in garnet of sample 12F03 (Fig. 10). Furthermore, the calculated contents of $X_{grs}$ and $X_{alm}$ that form the $X_{grs}$ shoulder and the step in $X_{alm}$ differ from the observed quantities by $\sim$0.04 and 0.03, respectively. In contrast to the observed garnet porphyroblast, the calculated rim of the second growth phase of garnet does not contain $X_{grs}$. The predicted absolute maximum in $X_{alm}$ differs from the observed $X_{alm}$ maximum by $\sim$0.03–0.04 depending on the heating rate applied for the simulation of garnet growth during the Cretaceous (Fig. 10). Except for the case, where the Cretaceous *P–T–t* loop is modelled with a heating rate of 5°C $Ma^{-1}$, the garnet growth simulations predict a significant $X_{alm}$ peak, which is not discerned in the investigated porphyroblast of rock sample 12F03 (Fig. 10).

Significant differences in the compositional gradients that result from variations of the heating rate applied for the Eo-Alpine metamorphic event can also be perceived at the transition between first and second garnet growth phase (Fig. 10). Whereas for simulations applying a heating rate of 100°C $Ma^{-1}$ a sharp compositional step is obtained even for $X_{sps}$ between first and second garnet growth phase, garnet growth modelling with heating rates smaller then 20°C $Ma^{-1}$ yields significantly smoothed compositional gradients.

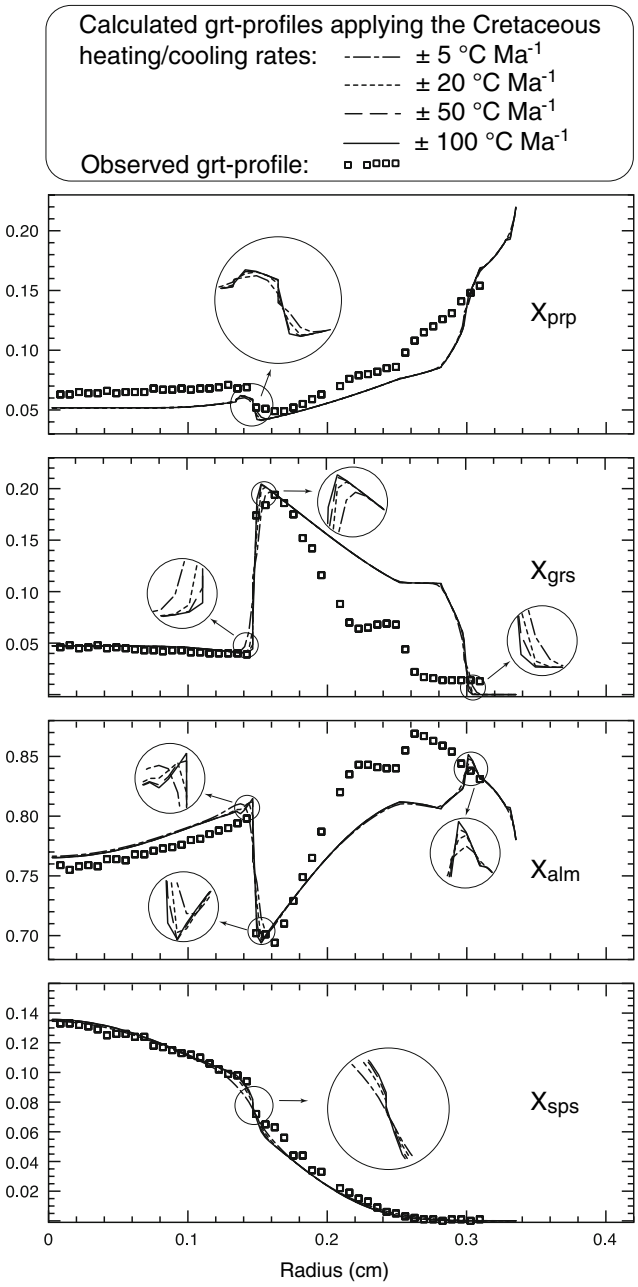


**Fig. 10** Compositional profiles of garnet from radius class 4 (Fig. 4) calculated for different heating/cooling rates during the Eo-Alpine metamorphic event in the Cretaceous. For the geothermal history during the Permian a heating/cooling rate of $\pm$ 3°C $Ma^{-1}$ and a maximum *T* of 675°C are considered. See the Appendix of Electronic supplementary material for detailed values of the *P–T–t* trajectories

## Discussion

The concentric chemical zoning and the homogeneous matrix that is devoid of chemical segregation in rock sample 12F03 are characteristic for the garnetiferous metapelites of the Wölz Complex. Both features indicate that chemical transport in the rock matrix was fast compared to the rates of garnet growth during the Permian and Cretaceous metamorphic events. In addition, the chemical zoning (Fig. 3; see also Fig. 5 of Gaidies et al. 2006) indicates that resorption of garnet that may potentially have occurred during phases of instability along the prograde part of the *P–T* path or during retrogression was minute and can be neglected when analyzing the compositional zoning pattern. Based on these notions, the rocks from the Wölz Complex lend themselves to the forward modelling of

garnet growth zoning with THERIA_G (Gaidies et al., 2007).

## P–T–t evolution of rock sample 12F03 obtained from garnet growth simulation

Even though the first garnet growth phase of the investigated garnet porphyroblast is 4 mm in diameter, garnet growth in the course of Permian metamorphism occurred over a comparatively small *P–T–t* range. This is explained by the large radial growth rate of garnet during the incipient stages of garnet growth (Gaidies et al., 2007). For the garnet growth simulation along *P–T–t* loop A$^{\star}$, this may lead to a garnet population density of $\sim$0.85 grt/cm$^3$ after a period of $\sim$2.8 Ma. Garnet crystals that originate from the fourth nucleation event are $\sim$3 mm in diameter. At the same time, garnet porphyroblasts that stem from the first nucleation event during the nucleation interval are $\sim$5 mm in diameter.

Simulation of garnet growth from $\sim$535°C up to 545°C (Fig. 11) at isobaric conditions of $\sim$3.8 kbar using a thermal maximum of 675°C and average heating and cooling rates of 3 and $-3$°C Ma$^{-1}$ during the Permian metamorphic cycle yields the best fit with the chemical zoning observed in the first garnet growth phase (Fig. 9). These results match the *P–T* conditions for the incipient stages of garnet growth in the Wölz Complex obtained in a previous study (Gaidies et al. 2006). From application of the isothermal fractionation model of Evans (2004), Gaidies et al. (2006) suggested a relatively flat *P–T* path for the formation of the first garnet growth phase, where *P* slightly increases with *T*.

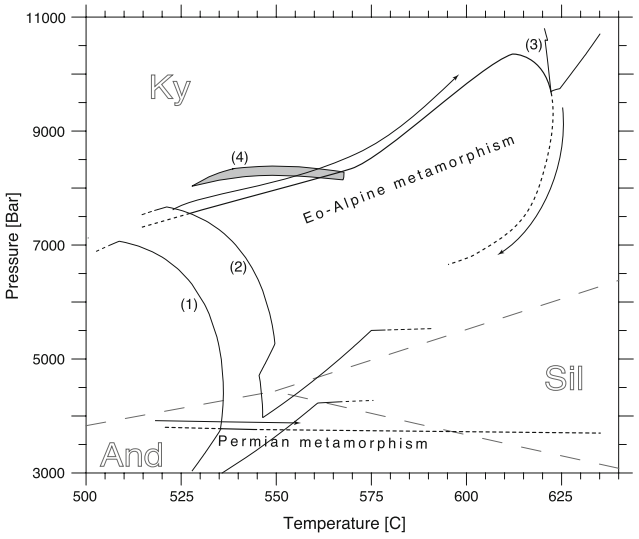


**Fig. 11** Polymetamorph *P–T* evolution of rock sample 12F03 obtained from garnet growth simulation (*unbroken lines*). (1) *P-T* conditions of incipient garnet growth during the Permian; (2) *P–T* conditions of incipient garnet growth during the Cretaceous considering an anti-clockwise Permian *P–T* loop; (3) low *P–T* conditions of garnet stability subsequent to garnet growth in the Cretaceous; (4) *P–T* conditions of the critical equilibrium assemblage, which have to be reached by the Eo-Alpine *P–T* trajectory (see text)

Mineral inclusions of ilmenite, quartz, and muscovite are observed in the first growth phase of garnet from rock sample 12F03 and are considered as parts of the equilibrium assemblages during Permian garnet growth. The first garnet growth phase and its inclusions represent the only remnants of Permian metamorphism in the rock sample. This assemblage is not diagnostic for the peak metamorphic conditions of the Permian event, and the question arises, whether the peak conditions can be constrained from garnet growth modelling.

A thermal maximum of 675°C for the Permian metamorphic event seems to conflict with the fine-grained rock matrix of sample 12F03. We hypothesise that the comparatively short-termed Eo-Alpine metamorphic event (Faryad and Chakraborty 2005) with peak conditions of $\sim$625°C at $\sim$10 kbar (Fig. 11) would not be able to reduce the size of all the coarse-grained matrix grains, which would have been formed in response to a previous metamorphic event with a thermal maximum of $\sim$675°C and a total duration of $\sim$150 My (Appendix of Electronic supplementary material). Coarse-grained minerals in addition to garnet are expected to be preserved as remnants of former *HT* metamorphic assemblages. Furthermore, pegmatite dykes, which are likely to be associated with such high-grade metamorphic rocks in the Austroalpine basement (e.g. Habler and Thöni 2001), are not known from the Wölz Complex. These findings contradict a thermal maximum of 675°C and rather point to a significantly lower maximum *T* for the Permian metamorphic event in the Wölz Complex.

A possible explanation for the discrepancy is the large uncertainty in the thermodynamic model and/or kinetic dataset. At this point, it must be noted that the requirements with respect to the accuracy of thermodynamic data are higher for garnet growth modelling than for conventional geo-thermobarometric methods and garnet isopleth thermobarometry. This is due to the fact that errors in the determination of the composition of the first garnet growth increment are propagated and possibly even amplified via the fractionation calculation. This may be problematic in particular for modelling of the late stages of garnet growth.

In the modelling presented here, pure $H_2O$ was considered as fluid phase. *P–T* phase diagram sections calculated for the bulk rock composition of rock sample 12F03 considering a graphite-buffered carbon-, oxygen- and hydrogen-bearing fluid (Connolly and Cesare 1993) indicate that at a pressure $< 6$ kbar the lower stability limit of garnet is shifted to lower temperatures by about 10°C compared with the respective

equilibrium-phase assemblage diagram calculated for pure $H_2O$ (Gaidies et al. 2006). At pressures exceeding 6 kbar, the influence of the fluid composition on equilibrium phase relations can be neglected. That is, the inappropriate description of the thermodynamic properties of the fluid may also contribute to the discrepancy between observed and calculated chemical composition of the first garnet growth phase.

Garnet isopleth thermobarometry applied to the early growth increments of garnet often yields *P–T* conditions that lie well above the calculated *LP/LT* stability limit of garnet (e.g. Gaidies et al. 2006; Stowell et al. 2001). This conspicuous discrepancy may either be due to reaction overstepping or it may simply be an effect of insufficient accuracy of the thermodynamic data. Yet an alternative explanation invokes modification of the original growth zoning through intragranular diffusion. Garnet isopleth thermobarometry is very sensitive to $X_{sps}$. According to thermodynamic modelling, $X_{sps}$ should be highest in the first garnet growth increments and it should decrease rapidly from the garnet-in curve into the garnet stability field. Manganese is the fastest diffusing component in garnet and it was shown by Gaidies et al. (2007) that it may effectively diffuse out of the garnet core and by this mechanism modify the original growth zoning.

Since the Permian garnet growth phase of rock sample 12F03 lacks inclusions of biotite, a possible anti-clockwise *P–T* trajectory during the Permian is merely hypothetical at this juncture. Moreover, because enhanced gradients in $X_{prp}$ and $X_{alm}$ at the outermost rim of the first garnet growth phase are not observed in garnet of sample 12F03 (Fig. 9), an anti-clockwise *P–T* loop seems unlikely. Therefore, we favour an isobaric to clockwise *P–T–t* trajectory.

The complex compositional pattern of the second garnet growth phase allows a detailed reconstruction of the geothermal history during Eo-Alpine metamorphism. In that respect, the shoulder in the $X_{grs}$ profile and the concomitant local maximum in $X_{alm}$, which are frequently observed in the central portion of the second growth phase of garnet porphyroblasts from the Wölz Complex, can be seen as a rock-specific geothermobarometer. From THERIA_G modelling, we infer that garnet growth started at ~530°C and ~7.6 kbar and ceased at ~623°C and ~9.7 kbar, which corresponds to the thermal maximum of the Cretaceous *P–T–t* trajectory (Fig. 11). Whereas the *T* calculated for incipient garnet growth during the Cretaceous matches estimates obtained by Gaidies et al. (2006), the *P* differs from what is proposed by the latter authors by ~0.7 kbar. Between ~586°C at ~9.1 kbar and ~595°C at ~9.6 kbar a period of garnet instability is found by THERIA_G modelling, at which garnet may have been subject to resorption. For the barometrical maximum of Eo-Alpine metamorphism a *P* of ~10.4 kbar is computed (Fig. 11).

Quartz, muscovite, ilmenite, rutile, plagioclase, and chlorite are calculated to have grown during the second metamorphic cycle. This is in agreement with petrographical observations. Furthermore, the growth simulations are consistent with a decrease in ilmenite and an increase in the modal amount of rutile towards the garnet rim. THERIA_G modelling predicts equilibrium assemblages with chloritoid between ~530°C at ~7.6 kbar to ~568°C at ~8.3 kbar (assemblages 5 and 6 in Fig. 5) and a staurolite-bearing assemblage for the range between ~595°C at ~9.6 kbar and ~605°C at ~10.1 kbar (assemblage 8 in Fig. 5). Chloritoid and staurolite are, however, not discerned in rock sample 12F03. Chloritoid should have been formed relatively early during the growth of the second garnet growth phase, and it is indeed frequently observed in the innermost portion of the Cretaceous growth phase of garnet porphyroblasts from the Wölz Complex. The lack of chloritoid at the respective position within the second growth phase of garnet from sample 12F03 may be explained by resorption of chloritoid in the course of garnet growth. Another possible explanation for the lack of chloritoid are shortcomings of the thermodynamic data.

Although predicted from calculated equilibrium phase relations staurolite probably was never present during Cretaceous garnet growth. For the stage where staurolite and garnet were in equilibrium with ilmenite, chlorite, (2)phengite, quartz, and $H_2O$ (assemblage 8 in Fig. 5) a significant maximum in $X_{alm}$ is predicted in the corresponding garnet growth increment for any feasible heating rates, i.e. for heating rates in excess of 5°C $Ma^{-1}$ (Fig. 10). However, such a feature is not perceived in the compositional profile of garnet.

From garnet growth modelling, average heating rates larger then 50°C $Ma^{-1}$ for the Eo-Alpine metamorphic event are likely. Only for such cases, the steep chemical gradients observed at the boundary between first and second garnet growth phase and particularly the sharp decrease of $X_{sps}$ can be reproduced numerically (Fig. 10). Hence, our results are compatible with the findings of Faryad and Chakraborty (2005) who obtained a heating rate of 100–260°C $Ma^{-1}$ for the Eo-Alpine metamorphic event.

Biotite, which is often observed as matrix mineral in rock sample 12F03 is not predicted to occur in garnet-bearing assemblages. The numerical simulations suggest its formation during the Permian metamorphic event subsequent to the growth of the first garnet phase (Fig. 7). For Eo-Alpine metamorphism biotite growth is suggested to have been occurred in the course of retrogression and decompression (Fig. 8). This may explain the small biotite flakes of the matrix crosscutting the rock foliation.

The large extent of garnet growth during the second metamorphic event compared with the first metamorphic episode can be explained by the specific *P–T* trajectory of Eo-Alpine metamorphism and the topology of the predicted equilibrium phase relations. For the geothermal histories investigated in this study (see the Appendix of Electronic supplementary material), the influence of internal metasomatism (Spear 1988) on phase equilibria in the interim between the Permian and Eo-Alpine metamorphic events is only minor.

### Limitations of garnet growth simulation

In principle, THERIA_G modelling may provide detailed information on the primary compositional gradients at the transition between the Permian and the Cretaceous garnet growth phase, which may be used as initial conditions for diffusion modelling. However, since the initial conditions are strongly contingent on the accuracy of the thermodynamic data, information on the temporal aspects of prograde metamorphism can still only approximately be determined.

Besides inaccuracies in the thermodynamic and kinetic databases, the departure of the calculated compositional profile of the second garnet growth phase from the observed chemical patterns may be explained by sluggish mass transport in the rock matrix. Such a scenario may be expected for the Cretaceous metamorphic event because the rocks were dehydrated significantly during Permian metamorphism. As a consequence, Cretaceous garnet growth may rather be seen as a competitive process between neighbouring garnet individuals (Carlson 1991).

In our growth modelling, all calcium-bearing matrix phases are exhausted during late stages of garnet growth, and the outermost portion of the second garnet growth phase is predicted to be free in $X_{grs}$. The fact that the outermost portions of the garnet porphyroblast of rock sample 12F03 have a low but readily detectable $X_{grs}$ content suggests that another calcium-bearing phase was present in the matrix also during the latest stages of garnet growth. Epidote and allanite are obvious candidates which have not been considered in the thermodynamic model.

It may be hypothesized that during the period of garnet instability between the Permian and the Cretaceous, the composition of the thermodynamically relevant bulk rock composition was changed. As possible mechanisms, resorption of garnet or fluid infiltration may be considered. However, because of the euhedral shape of the garnet grain and the satisfactory reconstruction of the oldest garnet growth increments that occurred during the Cretaceous, substantial resorption of the outermost portion of the first garnet growth phase is very unlikely.

## Conclusions

If local equilibrium can be demonstrated between the rim of a growing garnet and the rock matrix, the chemical zoning patterns of the garnet porphyroblast may provide geo-thermobarometric information on the entire garnet growth history. This information may be extracted from the observed zoning pattern by forward modelling of garnet growth with the THERIA_G software. For a given bulk rock composition the calculated zoning pattern is highly sensitive to the *P–T* trajectory, along which garnet growth is simulated. If intracrystalline diffusion is taken into consideration, this may even allow to constrain the timing of a specific metamorphic event. Both, slow heating and cooling rates as well as prolonged residence of the rock at elevated *T* tend to degrade compositional gradients that may be present in the original growth zoning. It is generally not possible to unravel detailed rate information from the zoning pattern of a garnet porphyroblast, but the integrated effects of *T* and *t* may be constrained.

With THERIA_G modelling many of the features of the complex compositional zoning observed in a garnet porphyroblast of rock sample 12F03 from the polymetamorphic Wölz Complex can be reproduced numerically. For this sample our garnet growth modelling yields an isobaric prograde *P–T* path at $\sim$3.8 kbar for the first garnet growth phase at low heating/cooling rates. This confirms the presumed *HT/LP* metamorphic event associated with lithospheric extension during the Permian. From the chemical zoning of the second garnet growth phase, constraints can be obtained on the geothermal history during Cretaceous garnet growth. Whereas for Permian metamorphism in the Wölz Complex a Buchan-type geothermal history is inferred, a Barrovian metamorphic event is documented for the Cretaceous. For the thermal maximum of Eo-Alpine metamorphism, *T* conditions of $\sim$625°C at $\sim$10 kbar are calculated. The maximum *P* yielded $\sim$10.4 kbar at $\sim$610°C, and average heating/cooling rates are estimated to be larger than $\pm$ 50°C $Ma^{-1}$ during the Cretaceous event.

The full potential of THERIA_G modelling can only be exploited, if detailed information on garnet CSD and mineral chemistry of the respective rock sample is available. In such case, the specific investigation of garnet grains that nucleated late in the geothermal history may provide well-founded estimates for the temporal aspects of prograde metamorphism. Furthermore, the improvement of thermodynamic data and further information on the kinetics of intragranular diffusion in garnet will essentially enhance the applicability of THERIA_G to natural rocks.

**Acknowledgments** The assistance of E. Reusser, W. Tschudin and R. Milke is gratefully acknowledged. Comments from S. Chakraborty, F. Spear and Editor J. Hoefs were very helpful.

## References


Abart R, Martinelli W (1991) Variszische und alpidische Entwicklungsgeschichte des Wölzer Kristallins (Steiermark, Österreich). Mitteilungen der Gesellschaft der Geologie- und Bergbaustudenten in Österreich 37:1–14

Atherton MP (1968) The variation in garnet, biotite, and chlorite composition in medium grade pelitic rocks from the Dalradian, Scotland, with particular reference to the zonation in garnet. Contrib Mineral Petrol 18:347–361

Bernhard F, Hoinkes G (1999) Polyphase micaschists of the central Wölzer Tauern, Styria, Austria. Berichte der Deutschen Mineralogischen Gesellschaft, Beiheft zum European Journal of Mineralogy 11:32

de Capitani C (1994) Gleichgewichts-Phasendiagramme: Theorie und Software. Berichte der Deutschen Mineralogischen Gesellschaft, Beiheft zum European Journal of Mineralogy 6:48

Carlson WD (1991) Competitive diffusion-controlled growth of porphyroblasts. Mineral Mag 55:317–330

Chakraborty S, Ganguly J (1992) Cation diffusion in aluminosilicate garnets: experimental determination in spessartine–almandine diffusion couples, evaluation of effective binary, diffusion coefficients, and applications. Contrib Mineral Petrol 111:74–86

Connolly JAD, Cesare B (1993) C-O-H-S fluid composition and oxygen fugacity in graphitic metapelites. J Metamorph Geol 11:368–378

Evans TP (2004) A method for calculating effective bulk composition modification due to crystal fractionation in garnet-bearing schist: implications for isopleth thermobarometry. J Metamorph Geol 22:547–557

Faryad SW, Chakraborty S (2005) Duration of Eo-Alpine metamorphic events obtained from multicomponent diffusion modeling of garnet: a case study from the Eastern Alps. Contrib Mineral Petrol 150:306–318

Faryad SW, Hoinkes G (2003) *P–T* gradient of Eo-Alpine metamorphism within the Austroalpine basement units east of the Tauern Window (Austria). Mineral Petrol 77:129–159

Feenstra A (1996) An EMP and TEM—AEM study of margarite, muscovite and paragonite in polymetamorphic metabauxites of Naxos Cyclades (Greece) and the implications of fine-scale mica interlayering and multiple mica generations. J Petrol 37:201–233

Franz G, Hinrichsen T, Wannemacher E (1977) Determination of the miscibility gap on the solid solution series paragonite–margarite by means of infrared spectroscopy. Contrib Mineral Petrol 59:307–316

Gaidies F, Abart R, de Capitani C, Schuster R, Connolly JAD, Reusser E (2006) Characterization of polymetamorphism in the Austroalpine basement east of the Tauern Window using garnet isopleth thermobarometry. J Metamorph Geol 24:451–475

Gaidies F, de Capitani C, Abart R (2007) THERIA_G: a software program to numerically model prograde garnet growth. Contrib Mineral Petrol. doi:10.1007/s00410-007-0263-z

Habler G, Thöni M (2001) Preservation of Permo-Triassic low-pressure assemblages in the Cretaceous high-pressure metamorphic Saualpe crystalline basement (Eastern Alps, Austria). J Metamorph Geol 19:679–697

Hejl E (1984) Geochronologische und petrologische Beiträge zur Gesteinsmetamorphose der Schladminger Tauern. Mitteilungen der Gesellschaft der Geologie- und Bergbaustudenten in Österreich 30/31:289–318

Hejl E (1998) Über die känozoische Abkühlung und Denudation der Zentralalpen östlich der Hohen Tauern - eine Apatit-Spaltspurenanalyse. Mitteilungen der Österreichischen Geologischen Gesellschaft 89:179–199

Holland TJB, Powell R (1998) An internally consistent thermodynamic data set for phases of petrological interest. J Metamorph Geol 16:309–343

Hollister LS (1966) Garnet zoning: an interpretation based on the Rayleigh fractionation model. Science 154:1647–1651

Loomis T, Ganguly J, Elphick S (1985) Experimental determinations of cation diffusitivities in aluminosilicate garnets. II. Multicomponent simulation and tracer diffusion coefficients. Contrib Mineral Petrol 90:45–51

Mandl G (2000) The Alpine sector of the Tethyan shelf—examples of Triassic to Jurassic sedimentation and deformation from the Northern Calcereous Alps. Mitteilungen der Österreichen Geologischen Gesellschaft 92:61–77

Schmid SM, Fügenschuh B, Kissling E, Schuster R (2004) Tectonic map and overall architecture of the Alpine orogen. Eclogae Geologicae Helvetiae 97:93–117

Schuster R, Frank W (1999) Metamorphic evolution of the Austroalpine units east of the Tauern Window: indications for Jurassic strike slip tectonics. Mitteilungen der Gesellschaft der Geologie- und Bergbaustudenten in Österreich 42:37–58

Schuster R, Thöni M (1996) Permian garnets: indication for a regional Permian metamorphism in the southern part of the Austroalpine basement units. Mitteilungen der Gesellschaft der Geologie- und Bergbaustudenten in Österreich 141:219–221

Schuster R, Scharbert S, Abart R, Frank W (2001) Permo-Triassic extension and related HT/LP metamorphism in the Austroalpine—Southalpine realm. Mitteilungen der Gesellschaft der Geologie- und Bergbaustudenten in Österreich 45:111–141

Schuster R, Koller F, Hoeck V, Hoinkes G, Bousquet R (2004) Explanatory notes to the map: metamorphic structure of the Alps—metamorphic evolution of the Eastern Alps. Mitteilungen der Österreichen Mineralogischen Gesellschaft 149:175–199

Sölva H, Thöni M, Grasemann B, Linner M (2001) Emplacement of Eo-Alpine high-pressure rocks in the Austroalpine Ötztal complex (Texel group, Italy/Austria). Geodinamica Acta 14:345–360

Spear FS (1988) Metamorphic fractional crystallization and internal metasomatism by diffusional homogenization of zoned garnets. Contrib Mineral Petrol 99:507–517

Spear FS (1993) Metamorphic phase equilibria and pressure–temperature–time paths. Mineralogical Society of America Monograph. Mineralogical Society of America, Washington, DC

Stowell HH, Taylor DL, Tinkham DL, Goldberg SA, Ouderkirk KA (2001) Contact metamorphic *P–T–t* paths from Sm–Nd garnet ages, phase equilibria modelling and thermobarometry: garnet ledge, south-eastern Alaska, USA. J Metamorph Geol 19:645–660

Thöni M (2002) Sm–Nd isotope systematics in garnet from different lithologies (Eastern Alps): age results, and an evaluation of potential problems for garnet Sm–Nd chronometry. Chem Geol 185:255–281

Thöni M (2006) Dating eclogite-facies metamorphism in the Eastern Alps—approaches, results, interpretations: a review. Mineral Petrol 88:123–148

Tollmann A (1985) Geologie von Österreich. Band 2. Ausserzentralalpiner Anteil. Deuticke, Wien

Vance D, Mahar E (1998) Pressure–temperature paths from *P–T* pseudosections and zoned garnets: potential, limitations and examples from the Zanskar Himalaya, NW India. Contrib Mineral Petrol 132:225–245

Vielzeuf D, Baronnet A, Perchuk AL, Laporte D, Baker MB (2007) Calcium diffusivity in alumino-silicate garnets: an experimental and ATEM study. Contrib Mineral Petrol 154:153–170

Zeh A (2001) Inference of a detailed *P–T* path from *P–T* pseudosections using metapelitic rocks of variable composition from a single outcrop, Shackleton Rang, Antarctica. J Metamorph Geol 19:329–350

Zeh A, Holness MB (2003) The effect of reaction overstep on garnet microtextures in metapelitic rocks on the Ilesha Schist Belt, SW Nigeria. J Petrol 44:967–994